IL NUOVO CIMENTO Vol. 33 C, N. 1 Gennaio-Febbraio 2010
DOI 10.1393/ncc/i2010-10562-8

Colloquia: ICTT2009

Adaptive mesh refinement techniques for diffusion-synthetic-accelerated discrete-ordinates neutral particle transport

J. Ragusa and Y. Wang
Texas A&M University - College Station, Texas 77843, USA

(ricevuto l' 1 Novembre 2009; approvato il 15 Gennaio 2010; pubblicato online il 2 Marzo 2010)

Summary. — An Adaptive Mesh Refinement (AMR) technique is presented for the one-group and the multigroup S_N transport equations discretized using a Discontinuous Galerkin (DG) method. A diffusion synthetic accelerator, also based on a DG discretization and directly obtained from the discretized transport equations, is given. Numerical results are provided for 2D unstructured triangular meshes.

PACS 28.41.Ak – Theory, design, and computerized simulation.
PACS 02.60.Cb – Numerical simulation; solution of equations.

1. – Introduction

The steady-state conservation statement for single-velocity neutral particles undergoing isotropic scattering in domain $\mathcal{D}$ is given by the linear Boltzmann equation [1]

$$(1)\quad \vec{\Omega}\cdot\vec{\nabla}\psi(\vec{r},\vec{\Omega})+\sigma_t(\vec{r})\psi(\vec{r},\vec{\Omega})=\frac{\sigma_s(\vec{r})}{4\pi}\int_{4\pi}\mathrm{d}\Omega'\,\psi(\vec{r},\vec{\Omega}')+q(\vec{r},\vec{\Omega})\quad\text{or}\quad\mathcal{L}\psi=\mathcal{H}\psi+q,$$

where ψ represents the angular flux. Standard notations have been used. In the S_N discrete ordinates methods, an angular quadrature set, $\{w_d,\vec{\Omega}_d\}$ $(1\leq d\leq N_d)$, is chosen, where N_d is the total number of directions [1]. The scalar flux is then computed as follows:

$$(2)\qquad \phi(\vec{r})\equiv\int_{4\pi}\mathrm{d}\Omega\,\psi(\vec{r},\vec{\Omega})\simeq\sum_{N_d}w_d\psi(\vec{r},\vec{\Omega}_d),$$

and Richardson's iteration (also referred to as Source Iteration, SI) is used to converge a numerical solution to eq. (1): $\mathcal{L}\psi^{\ell+1}=\mathcal{H}\psi^{\ell}+q$. To improve the iterative convergence, preconditioned versions of SI in the form of synthetic accelerations have been devised [2,3]. Typically, the S_N equations are spatially discretized using finite difference formulae or linear discontinuous finite elements. Even though the Discontinuous Galerkin Finite Element Method (DGFEM) was originally introduced to solve the neutron transport equation in the 1970s [4,5], its use to solve the neutron transport on unstructured

grids is much more recent [6-8]. In this paper, we apply a DGFEM technique to the S_N transport equations, focusing on Adaptive Mesh Refinement (AMR) and its interaction with synthetic acceleration for Richardson's iteration.

Mesh adaptivity is based on the fact that the solution does not exhibit the same smoothness throughout the computational domain. Hence, an appropriate and automated placement of mesh cells, resulting in a locally refined or adapted mesh, can yield a better accuracy of the numerical solutions with fewer unknowns. For the discrete ordinate method, a patch-AMR technique can be used and is based on a hierarchy of nested grids [9-12]. Patch-AMR can be relatively simple to implement in an already existing code that uses a fixed Cartesian grid. Some of the drawbacks may include the fact that the transport physics is not represented as closely as possible (the extent of refined patch being often too large), leading to more unknowns than necessary, and the need to converge inflow/outflow values in between nested grids (a feature not present in cell-based AMR). The authors of [9-12] employ the gradient of the scalar flux solution to drive the adaptive mesh refinement in 2/3D Cartesian geometries for a one-group (one-speed) transport equation; this gradient-based error estimator is known to be fairly accurate for low-order spatial discretization but is overly conservative for higher-order spatial schemes. In [13], a cell-based local refinement technique is described for S_N transport, where the value of the neutron mean-free-path (mfp) in a given cell is employed as a mesh refinement criterion. While this approach takes into account the size of potential internal layers at any given location in the domain, it does not account for the actual smoothness of the solution at these locations and is, therefore, not optimal. In [14,15], a two-solution concept is employed, where the difference between a fine solution and coarse solution is employed to determine local errors; the finer solution can be either computed using a higher-order approximation or a finer spatial grid.

In diffusive media, Richardson's iteration is known to be extremely slow to converge and diffusion-based preconditioning schemes are employed to accelerate the iterative solution. An effective diffusion preconditioner needs to be spatially discretized in a manner consistent with the spatial discretization of the transport equation [16, 3]; this typically results in diffusion schemes that are not symmetric positive definite (SPD) [17] and partially consistent schemes that retain the SPD nature of the diffusion operator are preferred in most cases. However, current synthetic accelerators are based on a continuous finite-element approximation in space and the use of AMR meshes can significantly increase the implementation complexity for such algorithms when multiple mesh refinement levels exist between neighboring elements for unstructured meshes. Here, we address the issue of the preconditioner's compatibility with AMR meshes.

In this paper, we employ a simpler spatial error indicator, based on the inter-element jump in the numerical solution, to drive the mesh adaptivity, utilize it within the DGFEM setting, devise a diffusion synthetic accelerator compatible with AMR meshes, and extend the methodology to energy multigroup approximation, where particles can have different speeds.

2. – Mesh adaptivity for DGFEM S_N transport

After angular and spatial discretization, eq. (1) can be represented in matrix form as: $\mathbf{L\Psi} = \mathbf{H\Psi} + \mathbf{q}$, where $\mathbf{L}$ is a block-diagonal operator (one block = one direction). Each block-diagonal of $\mathbf{L}$ can be ordered such that the spatial cells are visited from the inflow of the domain to its outflow in accordance with each direction $\vec{\Omega}_d$, and, due to the discontinuous nature of the spatial discretization, the numerical solution in each cell is

then a simple local solve. The inflow radiation for a given cell is obtained from its upwind neighbor (or the boundary condition when the cell lies on a boundary). Hence, matrix $\mathbf{L}$ is never formed nor stored, and only local cell inversions are required. This "matrix-free" technique for inverting $\mathbf{L}$ is commonly referred to as a transport sweep. The unit solve in transport sweeps consists in finding the solution in a given cell K; the DGFEM weak form for cell K and direction d is given by: Find $\psi_d \in V_p(K)$ such that $\forall b \in V_p(K)$

$$\left(\psi_d, (-\vec{\Omega}_d \cdot \vec{\nabla} + \sigma_t) b\right)_K + \left\langle \psi_d^+, b \right\rangle_{\partial K^+} = \left\langle \psi_d^-, b \right\rangle_{\partial K^-} + \left(Q_d, b\right)_K, \tag{3}$$

where b is a generic test function (of order p) and $\partial K^{\pm}$ are the outflow/inflow boundaries of element K. The traces $\psi^{\pm}$ are defined with respect to the outflow/inflow faces for direction $\vec{\Omega}_d$. $(\ ,\ )_K$ is the volume integral in $\mathbb{R}^m$ over element K and $\langle\ ,\ \rangle_{\partial K^{\pm}}$ denotes the surface integral (weighted by $|\vec{\Omega}_d \cdot \vec{n}|$) in $\mathbb{R}^{m-1}$, with m being the dimension of the geometry (here, $m = 2$). For additional discussion on high-order DGFEM applied to the S_N equations, refer to [8].

In order to prescribe the next adapted mesh on which the next numerical solution is to be computed, mesh adaptivity typically requires: 1) flexible geometrical data structures to handle the passing of information in between regions of various refinement levels, 2) local error estimates obtained from the current numerical solution and employed to assess the amount of error committed in a given cell, and, 3) projection/restriction operators to approximate data between cells of various refinement levels.

The initial mesh, $\mathbb{T}^0$, is typically a coarse triangulation of the domain. Once an element has been flagged for refinement, it becomes inactive and the child-elements are the new active cells. Refinement rules allow for a visit of the data tree structure. For 2D triangular meshes, a subdivision into four smaller triangular elements avoids the creation of sliver elements. The children elements and the parent element remain related and the refinement process leads to a hierarchy of mesh cells that have all been obtained from subdivisions of cells in the initial mesh $\mathbb{T}^0$. Once an element has been refined, it is removed from the sweep ordering and replaced by its children, in the appropriate order for all directions. Any level of refinement difference is allowed in between neighboring elements. The element-coupling algorithm is based on recursive calls to the function dealing with the 1-level refinement difference.

The fact that DG methods are discontinuous approximations, with the presence of jumps in the numerical solution at the interfaces between elements, can be used to monitor the approximation error. It has been observed that, as the mesh is refined, the magnitude of these jumps tends to zero, since the true solution is better approximated. Therefore, it is intuitive to monitor the jump values as an indication of the spatial error distribution. Additionally, the inter-element jumps are closely related to the interface residual used in the *a posteriori* error estimators in [18-20]. Strictly speaking, the jumps are direction dependent. However, 1) the angular information is often discarded after a transport sweep has been performed in a given direction and 2) the physical observable quantities are typically angle integrated. Thus, the information retained is usually limited to the angle-integrated quantities, and the following jump-based error indicator is used at adaptivity cycle k:

$$\eta_K^k \equiv \frac{\int_{\partial K} [\![\phi^k]\!]^2}{\|\phi^k\|_2^2} = \frac{\int_{\partial K} \left(\sum_d \left\{w_d [\![\psi_d^k]\!]\right\}\right)^2}{\|\phi^k\|_2^2}, \tag{4}$$

where $[\![a]\!] = a^+ - a^-$ is the jump definition. The criterion for refinement is as follows: an element K of $\mathbb{T}_h^k$ is selected for refinement if $\eta_K^k \geq \alpha \max_{K' \in \mathbb{T}^k}(\eta_{K'}^k)$, where α $(0 < \alpha < 1)$ is a user-defined fraction. This criterion allows to focus the computational effort on elements with the largest errors and tends to equi-distribute the spatial error. For one-speed transport problems, mesh adaptivity based on a DG approximation (of any order) simply requires that the inflow contribution for cell K, *i.e.* $\langle \psi_d^-, b \rangle_{\partial K^-}$, be properly computed. In the finite-element setting, the unknown ψ_d^- is also expanded on the basis comprised of the b functions in the upwind element and, therefore, the inflow contribution integrals require the calculation of a mass matrix in dimension $m-1$ when the problem's dimensionality is m. When the upwind element and element K have the same refinement level, this matrix is a standard square mass matrix. Using the fact that the finite element spaces are embedded, *i.e.* each basis function on any given mesh can be written as a linear combination of basis functions of its children cells, we can expand the restriction of a basis function in any coarser cell into the basis functions defined on a child cell. Hence, the inflow coupling mass matrix is, more generally, a rectangular square matrix. Such a coupling matrix needs only to be defined for the level-1 refinement difference; higher refinement level differences are treated in a recursive manner.

For energy-dependent particle distribution, the multigroup S_N equations

$$\left(\vec{\Omega}_d \cdot \vec{\nabla} + \sigma_t^g\right)\psi_d^g = q_d^g + \frac{1}{4\pi}\sum_{g'=1}^{G} \sigma_s^{g' \to g}\phi^{g'} \tag{5}$$

need to be solved. The application of mesh adaptivity in the multigroup setting requires that, for a given cell K, the volumetric scattering contributions from other energy groups be properly computed; in the finite-element setting, this involves the following integral $\left(\phi^{g'}, b^g\right)_K$. However, because material properties $(\sigma_t^g, \sigma_s^{g' \to g})$ can vary greatly between groups, so does the smoothness of the multigroup solution, and, group-dependent adapted meshes are utilized. The cross-group source contribution expressed in the previous integral requires, therefore, that a mass matrix in dimension m be computed. This matrix is the standard mass matrix when the basis functions in element K have the same refinement level in groups g and g'. Otherwise, it is a m-dimensional rectangular mass matrix, similar to the inflow contribution treatment. Examples of adapted meshes are provided in the results section.

3. – Synthetic accelerator compatible with adapted meshes

Since Richardson's iteration can be ineffective in diffusive media, a preconditioned version of it, based on a Diffusion Synthetic Acceleration (DSA) is employed. Typically, standard DSA schemes are based on a continuous finite-element approximation [6]. However, in the context of AMR meshes, this would require a considerable effort to treat hanging nodes for unstructured grids. Instead, we derive directly a stable and effective DSA scheme, starting from the discretized DGFEM S_N transport equations. The underlying functional for the DGFEM transport equations, $\Gamma(u, v) = \int_{4\pi}((\mathcal{H} - \mathcal{L})u + q, v)_{\mathcal{D}}$, is stationary at point $(\psi, \psi^\dagger)$, where $\psi^\dagger$ is the adjoint angular flux [21]. Γ is based on the weak form eq. (3) and contains the integration over the entire phase-space (*i.e.* the weighted sum over all directions, with w_d weights, and the sum over all cells K). The DGFEM diffusion approximation to the transport equation can be obtained using the following argument: in order to derive, in the diffusion setting, the best estimate

value for this functional at its stationary point, we restrict functions u and v to be linearly anisotropic in angle and specifically employ Fick's law from diffusion theory, *i.e.* we use $\psi(\vec{r},\vec{\Omega}) = \frac{\phi(\vec{r})+3\vec{J}\cdot\vec{\Omega}}{4\pi} = \frac{\phi(\vec{r})-3D(\vec{r})\vec{\Omega}\cdot\vec{\nabla}\phi}{4\pi}$ and a similar expression for $\psi^\dagger$; the diffusion coefficient is $D = \frac{1}{3\sigma_t}$. Note that we have explicitly made use of Fick's law ($\vec{J} \equiv \int_{4\pi} \mathrm{d}\Omega\, \vec{\Omega}\psi(\vec{\Omega}) \simeq -D\vec{\nabla}\phi$). After some lengthy algebra, the following DG diffusion formulation is obtained $b(\phi,\phi^\dagger) = l(\phi^\dagger)$, where the bilinear and linear forms are [22]

$$b(\phi,\phi^\dagger) = \left(\sigma_a\phi,\phi^\dagger\right)_{\mathcal{D}} + \left(D\vec{\nabla}\phi,\vec{\nabla}\phi^\dagger\right)_{\mathcal{D}} + \left(\kappa[\![\phi]\!],[\![\phi^\dagger]\!]\right)_{E_h^i} + \left([\![\phi]\!],\{\!\{D\partial_n\phi^\dagger\}\!\}\right)_{E_h^i} + \left(\{\!\{D\partial_n\phi\}\!\},[\![\phi^\dagger]\!]\right)_{E_h^i}, \tag{6}$$

$$l(\phi^\dagger) = \left(Q,\phi^\dagger\right)_{\mathcal{D}} + \left(J^{\mathrm{inc}},\phi^\dagger\right)_{\partial\mathcal{D}^r}. \tag{7}$$

where $\sigma_a = \sigma_t - \sigma_s$, $\{\!\{a\}\!\} = \frac{a^+ + a^-}{2}$, E_h^i is the set of interior faces (edges in 2D), and κ is a penalty coefficient. This form is akin to the DG Interior Penalty method [23] for the elliptic problem $\vec{\nabla}\cdot D\vec{\nabla}\phi + \sigma_a\phi = Q$. The main advantage of the above form over the standard continuous finite-element form is that 1) hanging nodes are naturally treated with a DG approximation and thus AMR transport can be accelerated with diffusion solves and 2) the form can easily be implemented in a "matrix-free" fashion, hence without the need for global matrix storage. This DG diffusion is SPD and is solved using a standard preconditioned conjugate gradient technique (with a typical Symmetric Successive Over Relaxation—SSOR—preconditioner). Finally, for details regarding how diffusion approximations can serve as a synthetic accelerator for transport solves, refer to [3].

4. – Results

The first example is taken from [24] (problem 4); left and bottom edges are reflective boundary conditions, top and right edges are vacuum boundaries. Two sources of equal strength are present in part of materials 1 and 2. Material 1 is a pure absorber, material 2 is a pure scatterer, and material 3 is quasi-void. The material distribution and initial mesh are shown in fig. 1(a). The solution and the adapted meshes at adaptivity cycles no. 6, 10, and 13 are given in figs. 1(b)–(d), respectively. The error *versus* the number of spatial unknowns for polynomial orders 1 and 4 is given in fig. 2(a) for both uniform refinement and the AMR approach. The error *versus* CPU time is provided in fig. 2(b). Clear, fig. 2 shows the effectiveness of AMR over uniform refinement, both in terms of wall-clock time and memory footprint. A higher-resolution AMR solution is used as reference solution to compute the error.

The second example is a multigroup (2-group) problem from [25] dealing with a shielded subcritical fissile configuration. The configuration is about 6 mean-free-path (mfp) thick in the fast neutron group (group no. 1), whereas it is about 20 mfp thick for the thermal group (group no. 2). Figure 3 shows the adapted meshes and their solution for both energy groups at adaptivity cycle no. 10, where we can clearly note that the differences in the spatial distribution of particle have been followed by the adapted computation (the shielding material has been clearly outlined in the thermal mesh).

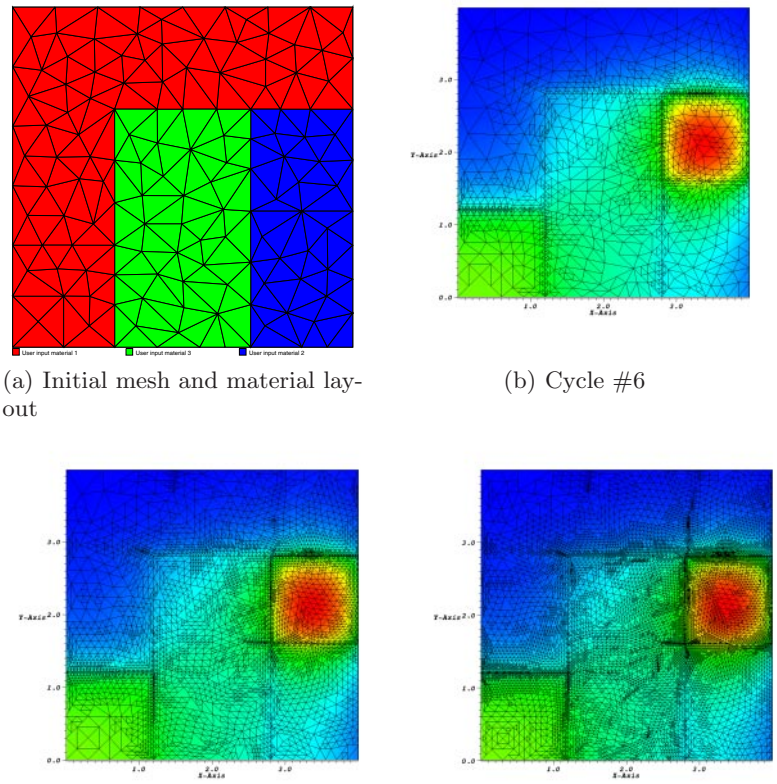

(a) Initial mesh and material layout

(b) Cycle #6

(c) Cycle #10

(d) Cycle #13

Fig. 1. – Material layout, solutions and adapted meshes for Example no. 1.

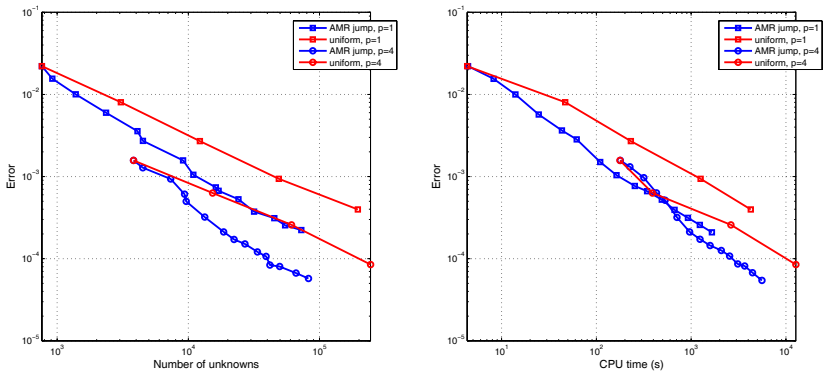

(a) Error *vs.* # of unknowns: uniform refinement and AMR

(b) Error *vs.* CPU time: uniform refinement and AMR

Fig. 2. – Example no. 1: convergence rates.

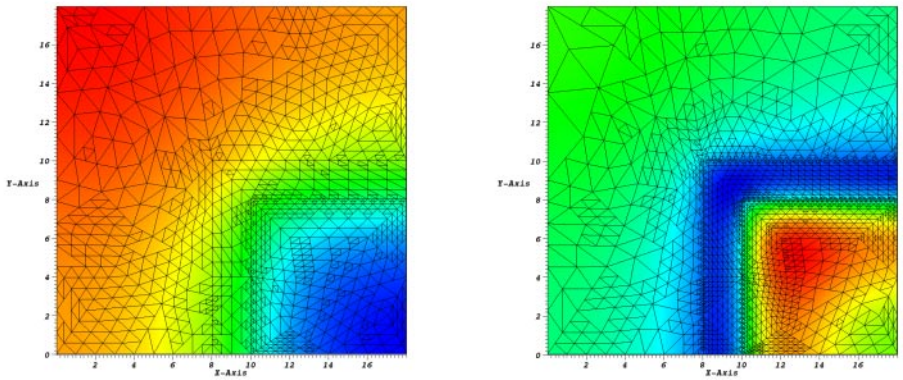

(a) Group #1 (b) Group #2

Fig. 3. – Solutions and adapted meshes at cycle no. 10 for Example no. 2.

5. – Conclusions and outlook

An Adaptive Mesh Refinement (AMR) technique has been presented for the one-group and the multigroup S_N transport equations discretized using a DGFEM. A DGFEM diffusion synthetic accelerator, compatible with AMR meshes, has been derived and given. Adaptivity has been performed for one-speed and multigroup problems. Numerical results for 2D unstructured triangular meshes show the benefits of adaptivity for neutral particle transport. Ongoing work includes the application of AMR techniques for S_N transport solvers to the Bolztmann-Fokker-Planck (BFP) equation for coupled electron-photon problems. The BFP equation can be effectively solved with standard S_N codes for neutral particles [26]. However, since electrons and photons have vastly different mean free paths, the AMR multigroup technique may prove even more beneficial for these simulations as we expect to capture boundary layer effects due to radiation and charged-particle non-equilibria at material interfaces. The extension to 3D AMR transport solves is also envisioned: for instance, the AMR sweeping graph should be constructed using the sweeping graph of the initial mesh and the child-parent elements' relations without the need to build a new graph at each AMR iteration, 3D element refinement rules should be prescribed to avoid sliver elements (*e.g.*, bisection of a cube/triangular-based prism (wedge)/tetrahedron element into 8 cubes/prisms/tetrahedra), and a face-based upwind procedure should be implemented (instead of edge-coupling used in 2D).

REFERENCES

[1] Duderstadt J. and Martin W., *Transport Theory* (Wiley, New York) 1979.
[2] Larsen E., *Transp. Theory Stat. Phys.*, **13** (1984) 107.
[3] Adams M. L. and Larsen E. W., *Prog. Nucl. Energy*, **40** (2002) 3.
[4] Reed W. H. and Hill T. R., Tech. Rep. Los Alamos National Laboratory LA-UR-73-479, Los Alamos National Laboratory (1973).
[5] P. L. and P. A. R., *On a finite element method for solving the neutron transport equation*, in *Mathematical Aspects of Finite Elements in Partial Differential Equations*, edited by deBoor C. (Academic Press, New York) 1974, pp. 89-123.

[6] Wareing T. A., McGhee J. M., Morel J. E. and Pautz S. D., *Nucl. Sci. Eng.*, **138** (2001) 256.
[7] Morel J. E. and Warsa J. S., *Nucl. Sci. Eng.*, **151** (2005) 157.
[8] Wang Y. and Ragusa J., *Ann. Nucl. Energy*, **36** (2009) 931.
[9] Jessee J. P., Fiveland W. A., Howell L. H., Colella P. and Pember R. B., *J. Comput. Phys.*, **139** (1998) 380.
[10] R. M. S., A. V. A., I. M. B., A. V. G., A. A. N. and V. Yu. R., *Different algorithms of 2d transport equation parallelization on random non-orthogonal grids*, in *Proceedings of Computational Methods in Transport, Granlibakken 2004*, edited by Graziani F., *Lecture Notes in Computational Science and Engineering*, Vol. **48** (Springer) 2006, pp. 235-254.
[11] Ogando F. and Velarde P., *J. Quant. Spectros. Radiat. Transfer*, **71** (2001) 541.
[12] Baker R. S., *Nucl. Sci. Eng.*, **141** (2002) 1.
[13] Aussourd C., *Nucl. Sci. Eng.*, **143** (2003) 281.
[14] Ragusa J. C. and Wang Y., *J. Comput. Appl. Math.*, **233** (2010) 3178.
[15] Duo J. and Azmy Y., *A posteriori error estimator and AMR for discrete ordinates nodal transport methods*, presented at the *International Conference on Reactor Physics, Nuclear Power: A Sustainable Resource, Interlaken, Switzerland, September 14-19, 2008* (American Nuclear Society, La Grange Park, IL) 2008.
[16] Alcouffe R. E., *Nucl. Sci. Eng.*, **64** (1977) 344.
[17] Warsa J. S., Wareing T. A. and Morel J. E., *Nucl. Sci. Eng.*, **141** (2002) 236.
[18] Führer C. and Kanschat G., *Computing*, **58** (1997) 317.
[19] Hartmann R., *Adaptive finite element methods for the compressible Euler equations*, Ph.D. thesis, University of Heidelberg (2002).
[20] Hartmann R. and Houston P., *SIAM J. Sci. Comput.*, **24** (2002) 979.
[21] Stacey W., *Nuclear Reactor Physics* (Wiley, New York) 2007.
[22] Wang Y., *Adaptive mesh refinement solution techniques for the multigroup S_N transport equation using a higher-order discontinuous finite element method*, Ph.D. thesis, Texas A&M University, College Station, USA (May 2009).
[23] Douglas J. and Dupont T., *Interior Penalty Procedures for Elliptic and Parabolic Galerkin Method*, *Lectures Notes in Physics*, Vol. **58** (Springer-Verlag, Berlin) 1976.
[24] Miller W. and Reed W., *Nucl. Sci. Eng.*, **62** (1977) 391.
[25] Smith M. A., Palmiotti G., Lewis E. E. and Tsoulfanidis N., *Nucl. Sci. Eng.*, **146** (2004) 141.
[26] Morel J. E., *Nucl. Sci. Eng.*, **79** (1981) 340.